Sustainability Analysis of Sandstone Using Smart Material by EMI Approach

Kushalendra Lal Kharwar (kushal05492@gmail.com)
MNNIT Allahabad: Motilal Nehru National Institute of Technology https://orcid.org/0000-0003-2252-4895
Anupam Rawat
Motilal Nehru National Institute of Technology
Rahul Srivastava
Government Engineering College Bharatpur

Research Article

Keywords: Structural health monitoring, EMI technique, Sensor system, Sandstone, Historical structure

Posted Date: September 2nd, 2022

DOI: https://doi.org/10.21203/rs.3.rs-1928320/v1

Sustainability analysis of sandstone using smart material by EMI approach

Kushlendra Lal Kharwar[1]· Anupam Rawat[1]· Rahul Srivastava[2].

Received: / Acceptance:

Abstract

In India, sandstone was broadly used to construct structures like Agra fort, Red Fort Delhi and Allahabad fort, etc. Around the world, many historical structures were collapsed due to the adverse effect of damages. Structural health monitoring (SHM) is very useful to take appropriate action against the failure of structure. The Electro-mechanical impedance (EMI) technique is used to continuously monitor the damage. This technique is helped to analyse the hairline crack, location, and severity of damage to structural elements. A 10cm length and 5cm diameter sandstone cylinder was used in experimental work. A cutter was used to create the artificial damages of 2mm, 3mm, 4mm, and 5mm respectively along the length, at the same place in specimens. The signature was measured for each depth of damage between 30 kHz to 400 kHz frequency range. The comparative result of healthy and damages state with different depth was concluded base on EMI signature form the sample. RMSD Statistical methods like root mean square deviation (RMSD) is used for quantification of damage. This paper motivates the application of the EMI technique to the historical building made of sand stone as key material.

Keywords Structural health monitoring, EMI technique, Sensor system, Sandstone, Historical structure.

Introduction

A lot of historical structures exist on the earth which contains the importance of history, civilization, symbols, etc. The historical structure contains comprehensive valuable history (Berrocal-olave et al., 2021). From ancient times, marble, sandstone, granite, wood, iron, limestone was used as construction material (Spectus, 2010). In India, there are a huge amount of ancient and historical structures (Dighe et al., 2020). The historical structure contains different construction materials, designs, and aesthetic, which is related to cultural diversity and religious diversity in India (Prakash & Rajdeo, 2019) (Pinna et al., 2022).

✉ Kushlendra Lal Kharwar
kushalkharwar@mnnit.aci.in

Anupam Rawat
anupam@mnnit.ac.in

Rahul Srivastava
er.me.rahul@gmail.com

1 Department of Civil Engineering, Motilal Nehru National Institute of Technology Allahabad, Prayagraj, 211004, India

2 Department of Mechanical Engineering, Government Engineering College, Bharatpur, Rajasthan, 321303, India

Many structures and forts containing Art, culture, and religious value were constructed during the period of the Mughal Empire. During this period, marble, and sandstone were widely used as construction material. Taj Mahal is an example of white marble, and Agra and Delhi fort are examples of various types of sandstone construction material. ‘Khusro Bagh’ was also constructed by sandstone, lime mortar etc. The ‘Khusro Bagh’ is a large walled garden complex located close to the Prayagraj Junction railway station, in Prayagraj district, Uttar Pradesh, India (Prasad et al., 2019). The four sandstone mausoleums within this walled garden, present an exquisite example of Mughal architecture. The structures are respectively tombs of Prince Khusro, tombs of Shah Begum, Khusrau's sister, Nithar, and tombs of Bibi Tamolan Khusrau's tomb was completed in 1622, while that of Nithar Begum's, which lies between Shah Begum's and Khusrau's tombs, was built on her instructions in 1624-25. Most of the structures in the Khusro Bagh are constructed with sandstone masonry (Figure 1 (a)). Red, brown, yellow, and white colour sandstone with lime mortar have been used in Khusro Bagh structures. Primarily large amount of red sandstone is used in these structures.

Sandstone is a natural sedimentary rock. It is available in a vast amount on the earth. Sandstone has been a prevalent construction material from ancient times to till now. The compressive strength and load-carrying capacity were high for sandstone as compared to other ancient construction materials. The sandstone has been used in beams, columns, domes, Mihrab arch, flooring, wall, fountains, etc., in structure. Sandstone is a hard rock that contains sand-size grains of mineral, sand, cementitious material, and organic material. The formation of sandstone is in two phases. In the first phase, sand particles sedimentation occurs through air or water; in the second phase, the compaction occurs with physical pressure and chemical changes. Variable colours are found in sandstone like red, black, brown, cream, dark-brown, yellow, pink, white, light and dark grey, etc. The colours of sandstone depend upon the mineral composition. These days' sandstone is broadly used in flooring, wall tiles, retaining wall, river training and stone masonry, etc. No painting is required after the use of sandstone. Sandstone has a fabulous construction material due to its shining, colour, and softness. The sandstone has been widely used in new construction structures i.e. Ambedkar Park Lucknow, Kashi Vishwanath corridor Varanasi, etc.

Archaeological structures and heritage sites located in India are exposed to the risks of environmental (Ural & Dog, 2008; Saba et al., 2018). Preserving cultural and architectural values and stability is very important. Many types of damage or deterioration occur in stone for various reasons in historic structures (Mahesh et al., 2021; Silva et al., 2022). The physical and chemical environmental, and loading impacts are significant causes of the deterioration of sandstone (Fermo et al., 2015). Different types of pollution threaten the existence of these historical structures and pieces of evidence (Varotsos et al., 2009). Pollution is a significant cause of the deterioration of historical structures like the white colour of the Taj Mahal marble has been going to yellowish colour due to the acid rain (Natarajan, 2022). Within two decades, the pollution is gradually rising due to the increasing size of vehicles, factories, workshops, thermal plants, refineries, and residential complexes (Belfiore et al., 2013). CO (Carbon monoxide) and SO_2 (Sulphur dioxide), are significant causes of deterioration of the sandstone in Gwalior Fort Madhya Pradesh (Pandey & Kumar, 2015). Rising damp in structural components and air pollution accelerates the deterioration of sandstone under the presence of NO_2 and SO_2 (Batista et al., 2019). Joerg Ruedrich et al. investigated the deterioration in sandstone under the weather conditions like wet-dry. They found the critical parameter is to increase the porosity in the sandstone indicator of deterioration (Ruedrich & Bartelsen, 2011). Akoğlu et al. investigated the swelling which play's important role for deterioration of sandstone under chloride environment. The micro crack increased the separation of layer especially along the bending plan, affect the deterioration in sandstone (Saltik, 2010). Rina (Irena) Wasserman was investigated the reason for sandstone deterioration was humidity, saltwater and high air pollution (Wasserman, 2021). Małgorzata Labus was investigated the deterioration and weight loss in sandstone under insolation, rain and frost (Labus and Bochen, 2012). J.J. Ortega-Calve et al. were investigated some bacteria is harmful to sandstone structure like cyanobacteria and chlorophytes that are present near the soil, plants, and surface of the structure (Ortega-calve and Ariiio, 1995). The leading causes of the deterioration in the historical building materials are air pollution, temperature, acid rain, salt water, and biological factor (Effectiveness et al., 2018) (Vidović et al., 2022).

Structural health monitoring (SHM) has been playing an important in preventing the abrupt failure of structures such as towers, bridges, dams, offshore structures, and buildings (Ai et al., 2014; Mishra, 2021). SHM techniques provide safety, reliability, of structure. SHM is one of the best effective industrialized methods for determining structural integrity. SHM techniques is helpful for recognize quality of structure, minor to major structural failure with an early indication of damage. Measuring the indication of the damage at an early stage through the SHM technique is to take appropriate action to prevent the damage before the collapse. It is a process to determine the presence, location, severity of damages present in the system, and also the remaining service life of the system. In SHM, various techniques are used to continuous or discontinuous monitoring and study the change in the behavior at any stage of the structure (Martínez-garrido and Ergenc, 2016). SHM is divided into two groups first is the global response technique, and the second is the local technique. In global technique contain static response and dynamic response technique. The global dynamic response technique is based on low frequency excitation and their vibration response like displacement, velocity, and acceleration, however global static response technique is based on only static displacement response. Mostly non-destructive evaluation (NDE) test is conducted to evaluate the change in the structural parameters. The local damage in structural members plays a hostile role in the structure. Many non-distractive tests, such as Ultrasonic, X-rays, Eddy current, Magnetic particle, Dye penetrant, EMI technique, etc., are conducted to evaluate the performance of damages in members of the structure (Maurya et al., 2020). The limitation of these techniques is less sensing range, and most of the method depends on the geometry, material properties, and depth of cracks, etc. The minimum and maximum probability sensitive range of the local technique are provided in table 1.

The EMI technique is comparatively new in SHM. Last few decades, this technique has been used in buildings, bridges, railways, towers, etc., for monitoring purposes. EMI technology based on the piezoelectric ceramic (PZT) sensor has versatile potential applications in SHM (Dongyu et al., 2014; Bhalla & Soh, 2004a). The PZT sensors were used as embedded or surface-bonded inside the host specimens (Maurya et al., 2022a). The surface-bonded sensor applied at the surface with the help of high epoxy adhesive (Moharana & Bhalla, 2014; Saravanan & Chauhan, 2022). The embedded sensor is used inner part of the host structure (Negi et al., 2018). The PZT sensor effectively monitors and detects incipient damage (Shanker et al., 2011). The incipient damage influences the strength and sustainability of structural members. This technique helps determine the incipient damage of structural elements. The PZTs sensor are also used in global dynamic response technique below the frequency range 100 Hz. The use of the EMI technique in aerospace and automobile sectors indicates the change in function during the operational process and any chance of malfunction. The PZT sensor is also used in parallel and series combination (Priya et al., 2018).

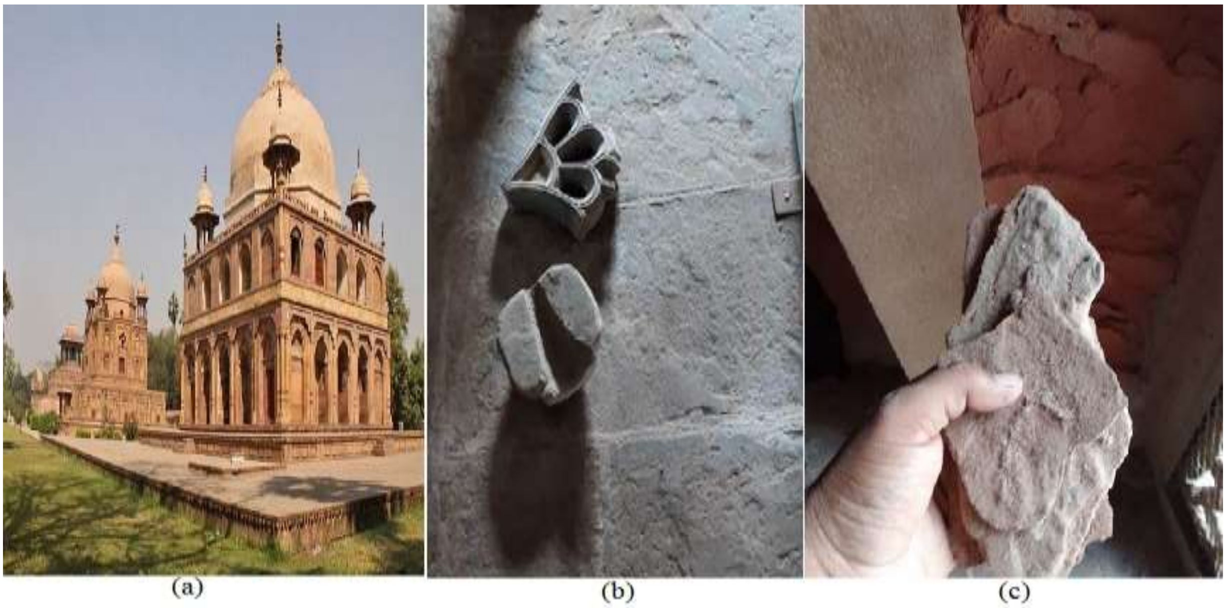

Fig. 1 (a) Historical structure Khusro Bagh, (b) and (c) Sample collection of Khusro tombs

Table 1 Sensitivity range of common local techniques (Bhalla 2004)

S.	Name of Local Technique	Minimum probability detectable crack length	Maximum probability Detectable crack length (>95%)	Remarks
1	Ultrasonic pulse velocity	2mm	5-6mm	Depends upon the properties and geometry of material
2	X – Ray	4mm	10mm	Dependent upon Structural Member configuration. Better for thickness of member is grater then 12mm
3	Magnetic particle	2mm	4mm surface	--
4	Dye penetrant	2mm	10mm surface	--
5	Eddy currents (At low frequency)	2mm	4.5-8mm	Thickness of testing specimen <12mm only
6	Eddy currents (At high frequency)	2mm for surface and 0.5mm for bore holes	2.5 mm for surface and 1.0mm for bore holes	--

Environmental impact on historical structure

Environmental impact on sandstone structure is a lengthy and time taken process. Acid water, temperature, pressure, wet-dry, humidity, freeze-thaw, etc., are significant causes of deterioration of historical structures under the environmental impact (Batista et al., 2019; Manohar et al., 2020). The porosity participates in the deterioration of stone due to environmental effects. The variation of temperature with sudden rainwater is very harmful to structure.

The shrinkage and swelling is a major process of deterioration of historical stone structure. The porosity of stone rock plays a vital role in durability. The deterioration rate of stone depends upon the porosity; damage or deterioration rises gradually when porosity increases. Figure 2 (a), (b), (c), and (d) contain the deterioration of sandstone in the Khusro tombs structure.

Loading impact on historical structure

The loading impact on historical structure cause by dead load, live load, earthquake load, wind load, vibration loads. Generally, no new construction occurs on historical structure due to no change in historical originality, so the dead load does not increase. Mostly the vibration load and earthquake loads are very harmful as compared to other loads. Now a day development is a need of every city. The rate of growth of the infrastructure of the city is very high. The need of human being in the city is the metro, multi-story building, water tank, water supply line, electricity and mobile tower, and railway line and station. New construction near the historical site produces vibration due to transport systems, electrification, water supply line, tower, bridges, metro, railway etc. The heavy vibration equipment in the construction industry produces vibration, which harms the stability of the historic structure.

Materials and Methods

Experimental work

The PZT-5H square sensor of 1 × 1 cm is manufactured by Ceramic India Ltd. The properties of the PZT-5H sensor are given in table 2. This PZT sensor has contained both nodes on the upper surface. A special type of low resistance single core wire of one meter was attached to PZT nodes. A smooth surface sandstone specimen of 10 cm in length and 5cm in diameter have been used for testing collected from the Khusro tomb. The center of specimen diameter is also the center of PZT patch. The high-strength epoxy has been used to attach the PZT sensor to the sandstone surface. A LCR meter is used to measure the signature conductance and susceptance. One end of the wire attached with PZT electrode and another end of this wire is connected with an LCR meter. To analyze the sustainability of sandstone, the manual damage has been created along the length at depths of 2mm, 3mm, 4mm, and 5mm respectively, at the same place in specimens with the help of a cutter. Figure 3 is the experimental test setup for testing in the laboratory.

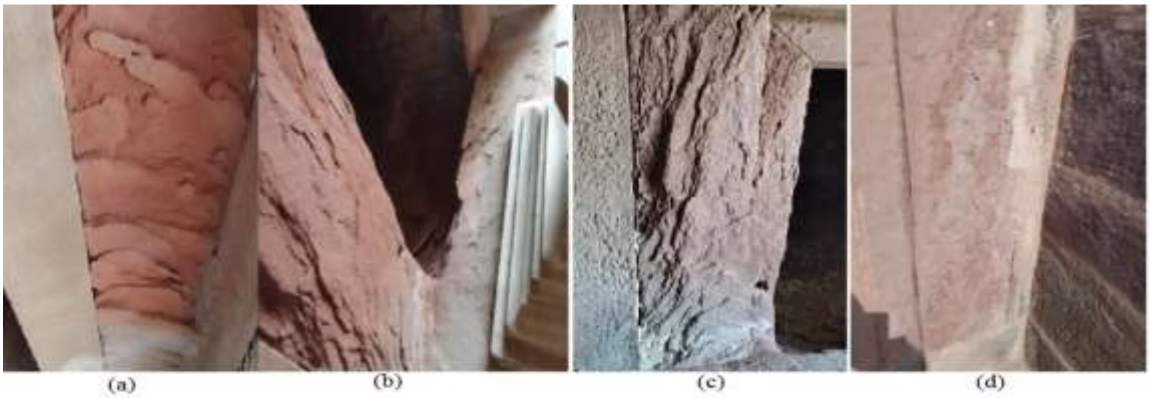

Fig. 2 (a), (b), (c), and (d) Deterioration of sandstone in Khusro tombs structure

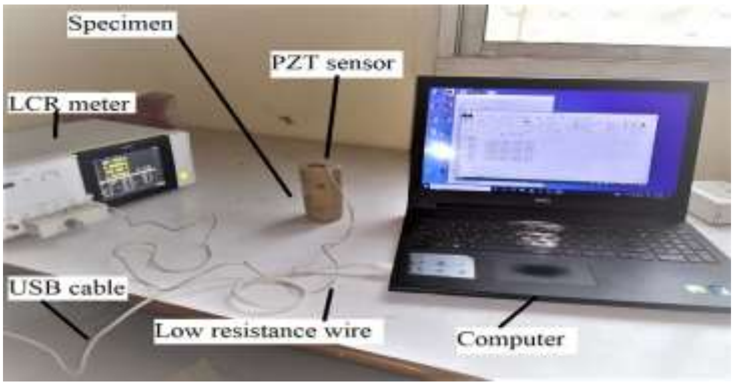

Fig. 3 Experimental test setup

Properties of sandstone

The sandstone is a sedimentary rock that forms by clastic sedimentation of sand, minerals, organic compounds, cementitious, matrix material. The size of grains of minerals ranges from 0.06 to 2 mm and wide range of the strength from less than 5.0 MPa to over 150 MPa. The strength is depending upon the porosity, cementitious material, matrix material, grain size, composition. In this experimental the sandstone sample made by the collected sandstone from tombs of Prince Khusro in figure1 (a), (b), and (c). A lithological characteristics studies of sandstone sample have been conducted. The sample is characterized by non-bedded structure; it is compacted in nature. It is containing Quartz and orthoclase. The rock has clastic texture. Subordinate amount of muscovite mineral is present

Damage in sandstone

The volumetric change in the original objects is called deterioration/damage. There are many causes of damage in sandstone like environmental and loading impact (Korkanç, 2013). The environmental deterioration is gradual deterioration. Small pieces erosion of sandstone are spall out from in the structure when the surface deterioration starts in sandstone. The depth of damage increases when the material spalls out from the structure. In this experimental work the depth of damage is gradually increase up to 5mm depth. A cutter was used to create the artificial damages in the specimen along the length. The damage depth is 2mm, 3mm, 4mm, and 5mm.The signature has been measured at every depth of damage (figure 4 (a), (b), (c), and (d)).

Fig. 4 (a), (b), (c) and (d) are 2mm, 3mm, 4mm, and 5mm depth of damage respectively.

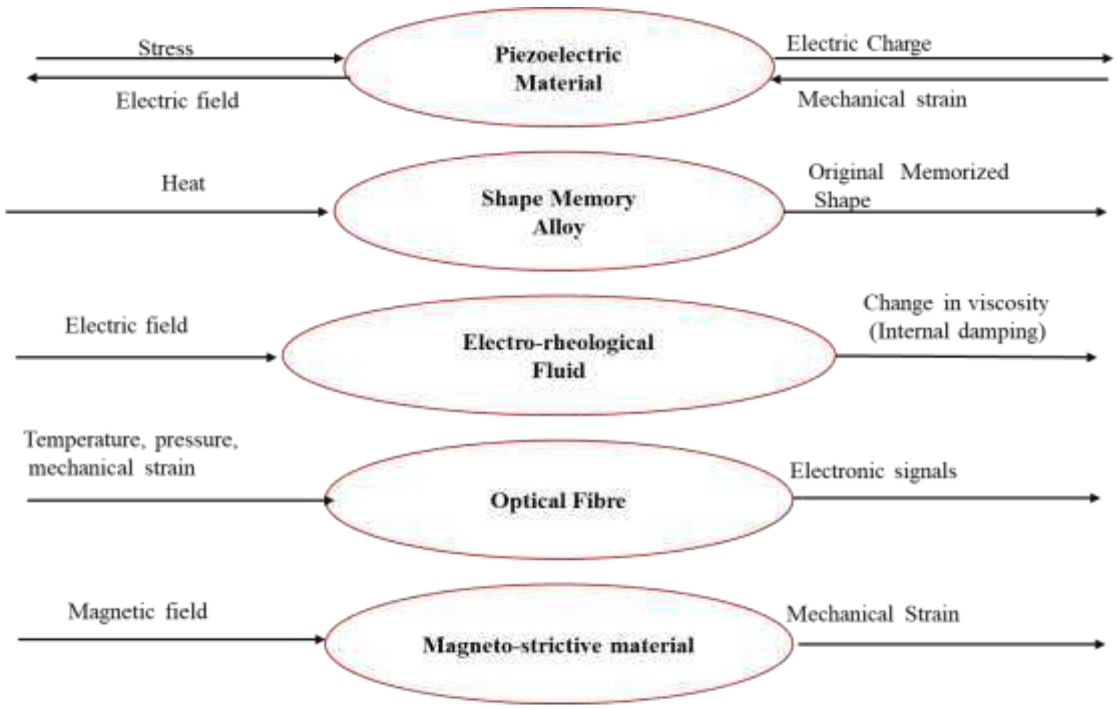

Fig. 5 Common smart materials: applications and the associated stimulus-response.

Piezoelectric materials

Some unique crystal materials like PZT [Pb (Zr1-xTix) O_3], PLZT [(Pb1-xLax) (Zr1-yTiy) O_3)], lithium Niobate (LiNbO3), and quartz (SiO2), etc., have the piezoelectric effect. These types of crystal is also called non-centrosymmetric crystals. The chemical composition of piezo-ceramic is [Pb (Zr1−xTix) O_3]. Generally, the piezo-ceramic is called PZT. PZT has an interesting smartness when the voltage applied on PZT it generates mechanical force and, when it is subjected to mechanical force, becomes electrically polarized. PZT is a smart material that have dual character, sensor as well as an actuator (Shanker et al., 2011). Various types of PZTs patches are commercially available such as specification, sensing frequency range, and shapes. Figure 6 is an experimental PZT patch having a size of 1cm×1cm.

$$D_i = \varepsilon_{ij}^{\bar{T}} E_j + d_{im}^{d} T_m \quad 1$$

$$S_k = d_{jk}^{c} E_j + s_{km}^{\bar{E}} T_m \quad 2$$

Where equation 1 is direct effect and equitation 2 is converse effect. The equations 1 and 2 can be rewritten in the tensor form as equation 3 (Sirohi & Chopra, 2000).

$$\begin{bmatrix} D \\ S \end{bmatrix} = \begin{bmatrix} \overline{\varepsilon^{T}} & d^{d} \\ d^{c} & s^{\bar{E}} \end{bmatrix} \begin{bmatrix} E \\ T \end{bmatrix} \quad 3$$

Where (D) is the electric displacement vector quantity [3x1] and unit is (C/m^2), (S) is the second order strain tensor [3x3], (E) is applied external electric field vector [3x1] and unit is (V/m).T is stress tensor [3x3] and unit is (N/m2).

(ε) is di-electric permittivity. ($\overline{\varepsilon^{T}}$) is the second order dielectric permittivity tensor under constant stress and unit is (F/m), (dd) and (dc) is the third order piezoelectric strain coefficient tensors and unit is respectively (C/N), (m/V). ($\overline{s^{E}}$) is fourth order elastic compliance tensor under constant electric field and unit is (m2/N).

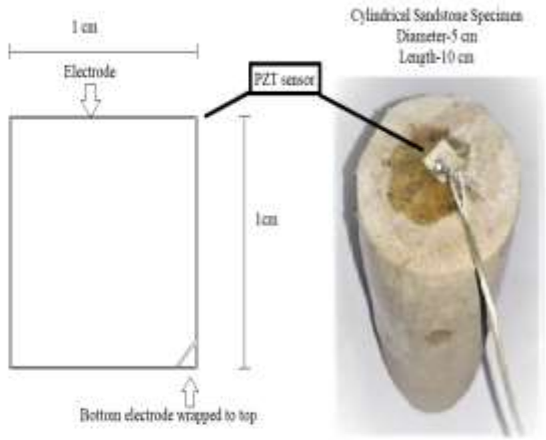

Fig. 6 Sandstone testing sample surface bonded with PZT sensor.

Table 2 Properties of PZT-5H sensor

Properties	Symbol	Units	Value
PZT thickness, m	t	0.003	PZT thickness, cm
PZT size, cm x cm	‘l’ and ‘w’	0.01 x 0.01	PZT size, m x m

Young's modulus	Y^E		6.4
Density		(g/cm3)	7.45
Piezoelectric Charge (Displacement Coefficient)	d31,d32	Coul/N x 10-12	-186
Piezoelectric Charge (Displacement Coefficient)	d33	(pC/N)	670
Piezoelectric Charge	d15	(pC/N)	660
Electric permittivity, x 10-8	$\varepsilon_{11}^T = \varepsilon_{22}^T$	F/m	1.750
Electric permittivity, x 10-8	ε_{33}^T	F/m	2.124
Mechanical loss factor	η	-	0.0325
Dielectric loss factor	δ	-	0.02
Poisson's	μ	-	0.31

EMI technique

EMI technique is NDE method. In the EMI technique, a PZT patch is used to monitor the health of the structure within a specific range of frequency. The EMI technique is similar to the global dynamic response techniques. In the global dynamic response technique, the frequency range works less than 100 Hz. Within 100Hz frequency is not suitable for incipient and hairline damage (Maurya et al., 2022b). The incipient and hairline damage evaluation and repair are necessary to prevent the big failure. The EMI technique is helpful to the measure the incipient damage, severity, and location of damages. The difference between in global dynamic technique and EMI is the frequency range. EMI technique works on 30 kHz-400 kHz frequency range. An LCR meter or impedance analyzer is used to acquire the signature. The LCR meter measures the admittance which consists of the real part (conductance) and imaginary part (susceptance), when plotted as a function of frequency, gives a unique signature to structures.1-D and 2-D expressions of electromechanical admittance, written below in equations 4 and 5 respectively.(Consumption, 1994; Bhalla & Soh, 2004a, 2004b).

$$\bar{Y} = G + Bj = 2\omega j \frac{wl}{h}\left[\left(\overline{\varepsilon_{33}^T} - d_{31}^2\overline{Y^E}\right) + \left(\frac{Z_a}{Z+Z_a}\right) d_{31}^2\overline{Y^E}\left(\frac{\tan kl}{kl}\right)\right] \quad 4$$

$$\bar{Y} = G + Bj = 4\omega j \frac{l^2}{h}\left[\left(\overline{\varepsilon_{33}^T} - \frac{d_{31}^2\overline{Y^E}}{1-\nu}\right) + \left(\frac{Z_{a,eff}}{Z_{s,eff}+Z_{a,eff}}\right)\frac{d_{31}^2\overline{Y^E}}{1-\nu}\bar{T}\right] \quad 5$$

Where $\bar{Y}$ is complex electromechanical admittance, G is conductance, B is susceptance, Z is mechanical impedance, Za is mechanical impedance of the PZT patch, d is piezoelectric strain coefficient, ω is angular velocity, l is half-length of PZT patch, h is thickness of PZT patch, w is width of PZT patch,, ε is electric permittivity, $\overline{\varepsilon_{33}^T}$ is complex electric permittivity at constant stress, $\overline{Y^E}$ is complex Young's modulus of elasticity at constant electric field, k is spring constant, ν is Poisson's ratio, $\bar{T}$ is complex tangent function, $Z_{a,eff}$ is effective impedance of the PZT patch, $Z_{s,eff}$ is effective impedance of the structure, j =$\sqrt{-1}$.

Major findings

The variation of conductance has been measured, such as the conductance signature of health state and at damage depths of 2mm, 3mm, 4mm, and 5mm, respectively. All conductance signatures are shown compared with healthy state conductance signatures in Figures 7, 9, 11, 13, and 15.

The susceptance signature is imaginary part of the admittance. The variation of susceptance signature is very slight as compared to the conductance signature. The susceptance signature has been measured at a healthy state and various damage depths such as 2mm, 3mm, 4mm, and 5mm, respectively, which are in figure 8, 10, 12, 14, and 16.

A comparative signature of conductance at the healthy state with various depths of damage has been in Figure 17.

A comparative signature of susceptance at the healthy state with various depths of damage has been in Figure 18.

Shifting the signature curve towards the left side from the baseline indicates the damage in the specimen. The shifting of curves was directly dependent upon the depth of damage when the depth of damage increases then the shifting towards the left side in conductance and susceptance signature. The change in the 5 mm damage signature is high compared to other signatures.

The percentage RMSD value is used for the evaluation of the damage. The percentage RMSD values was calculated for conductance and susceptance was shown in figure19.

With the help of conductance and susceptance percentage, curve of RMSD value is plotted in figure 20.

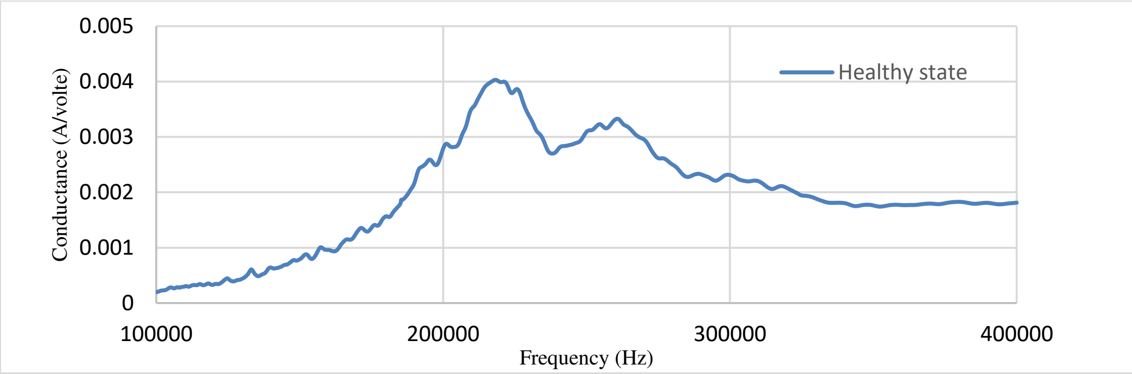

Fig. 7 Healthy state conductance/Frequency signature**.**

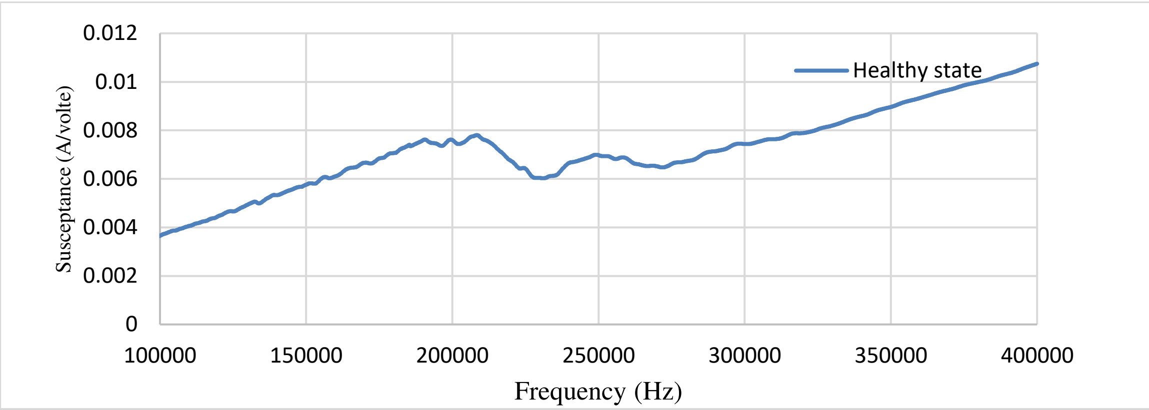

Fig.8 Healthy state susceptance/ Frequency signature.

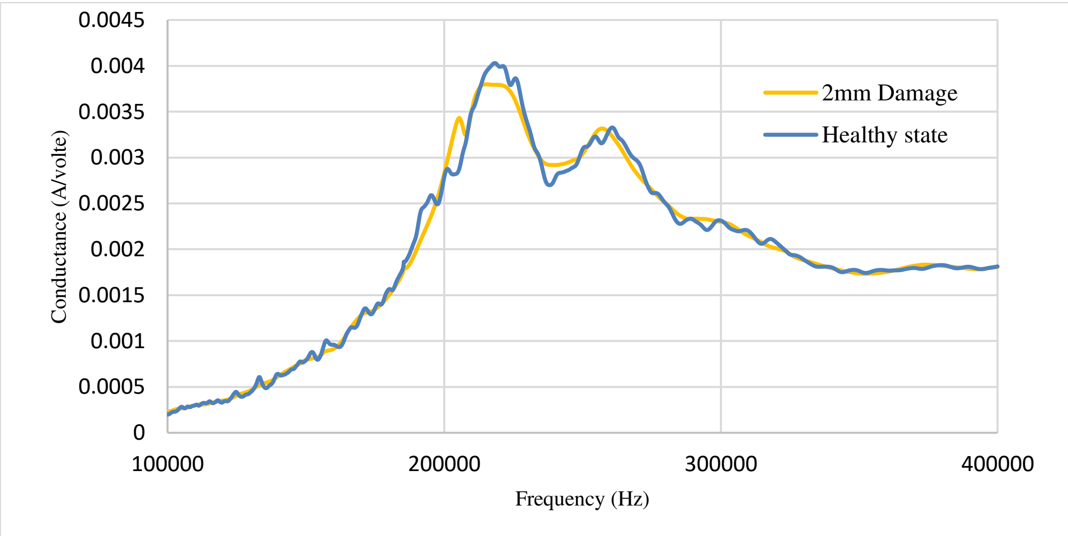

Fig 9. 2 mm Damage-conductance/Frequency signature

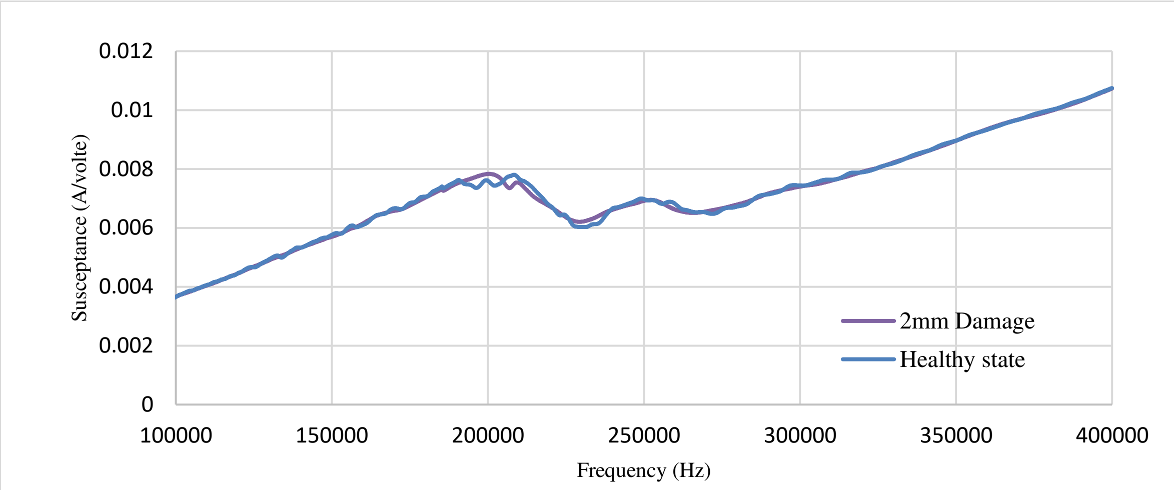

Fig.10 2mm Damage - susceptance/ Frequency signature

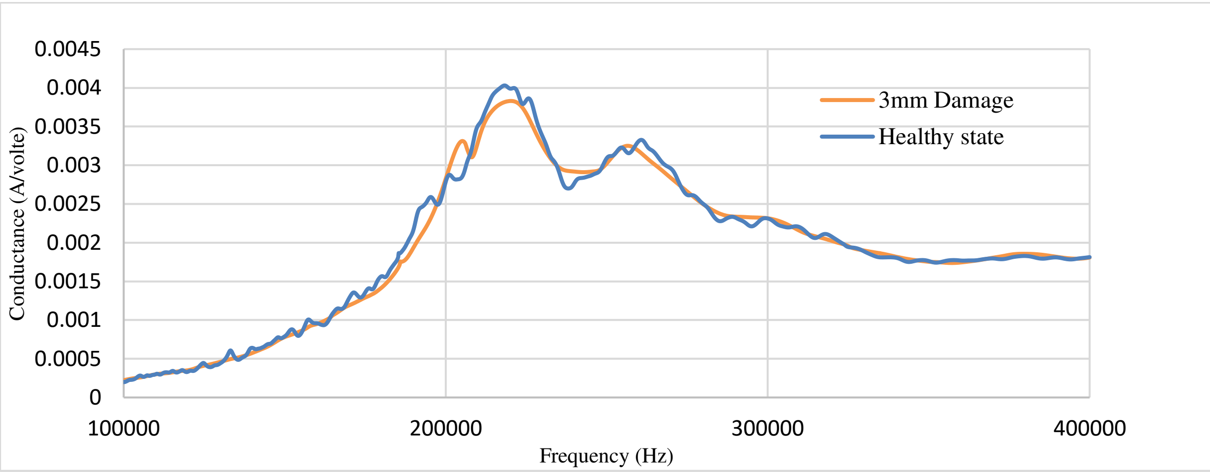

Fig. 11 3 mm Damage-conductance/Frequency signature

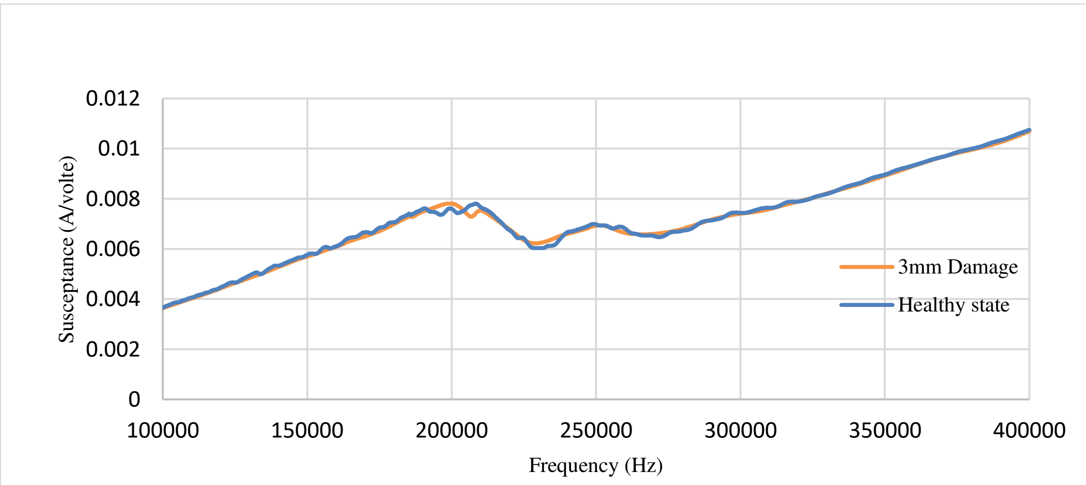

Fig.12 3mm Damage - susceptance/ Frequency signature

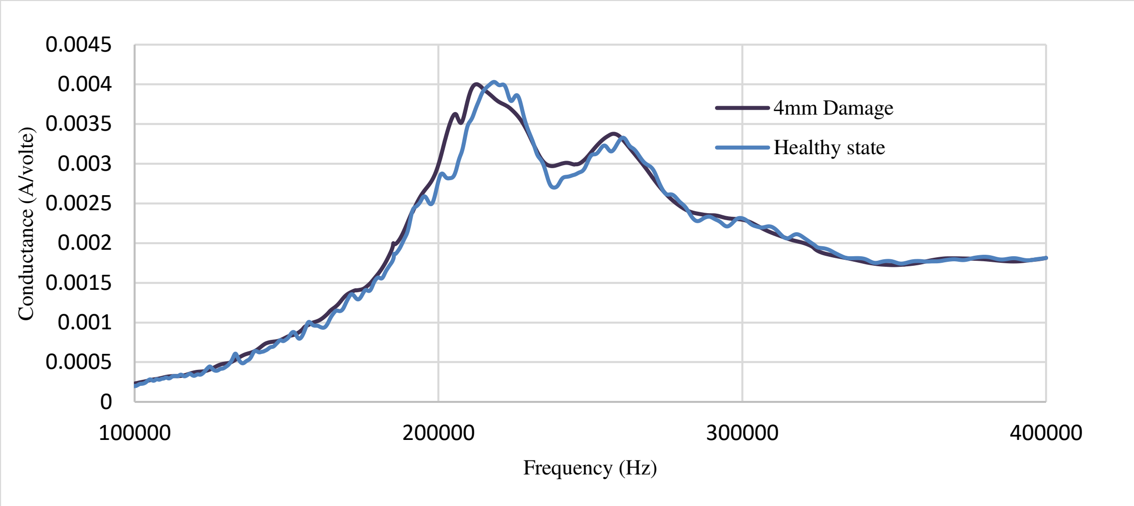

Fig. 13 4 mm Damage-conductance/Frequency signature

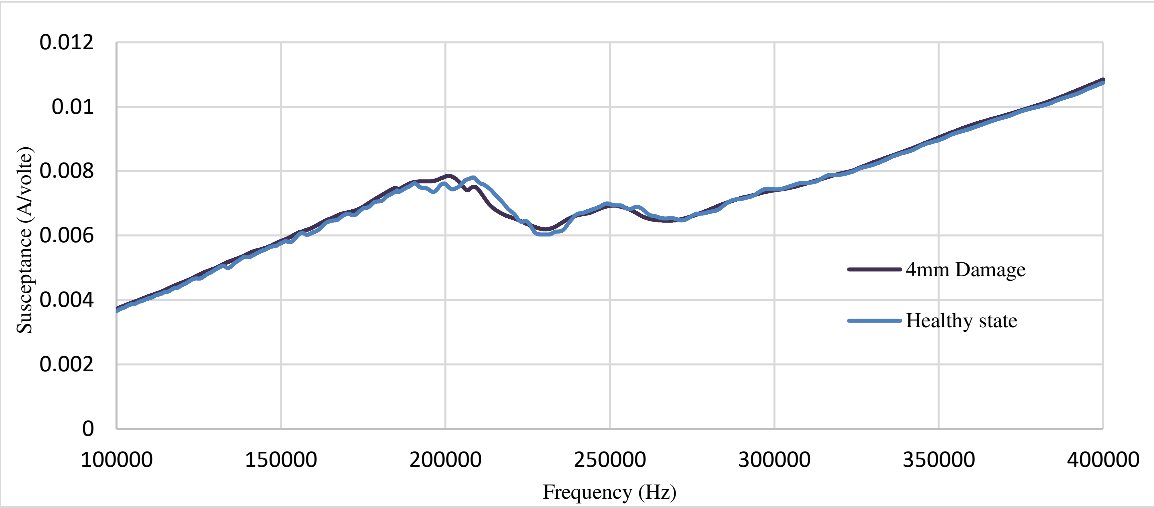

Fig.14 4mm Damage - susceptance/ Frequency signature

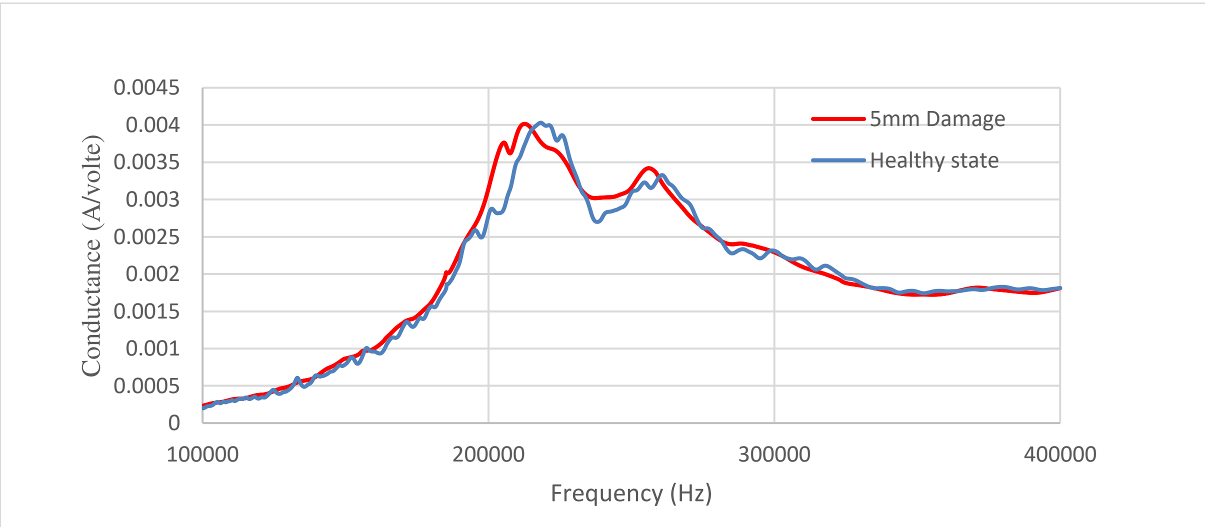

Fig. 15 5 mm Damage-conductance/Frequency signature

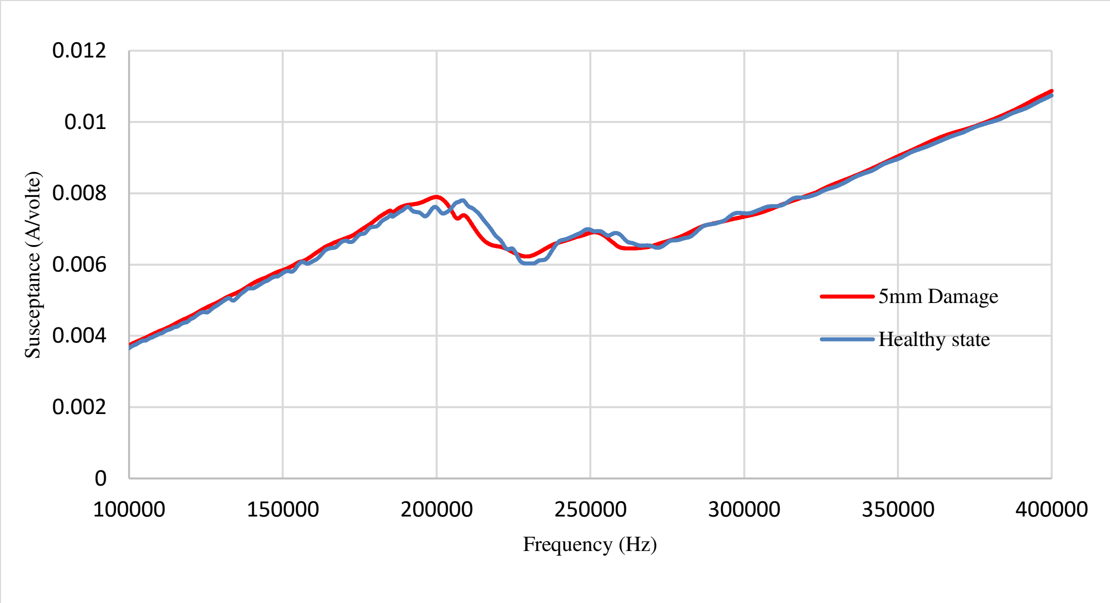

Fig.16 5mm Damage - susceptance/ Frequency signature

Evaluation of conductance and susceptance signature

The purpose of the evaluation is co-related with structural functions like strength gain and losses, damage, early strength change, etc. There are serval statistical methods like RMSD, mean absolute percentage deviation (MAPD), covariance (Cov), and correlation coefficient (CC) is used to evaluate the damage. The RMSD value is calculated with the help of conductance and susceptance signature. In the EMI technique, the RMSD is widely used to assess the damage's severity. The severity of damage is estimated by the amount of variations between two conductance and susceptance signatures. The equitation of percentage RMSD is written in equitation number 5.

$$\text{RMSD (\%)} = \sqrt{\frac{\sum_{i=1}^{N}(G_i^1 - G_i^0)^2}{\sum_{i=1}^{N}(G_i^0)^2}} \times 100 \qquad 5$$

The variation of conductance and susceptance both are calculated individual. A significant change was found in RMSD value of conductance signatures compared to RMSD values of susceptance signature. The RMSD value of conductance and susceptance at different depths of damage is shown in figure 19. The equitation of percentage RMSD is shown in figure 20.

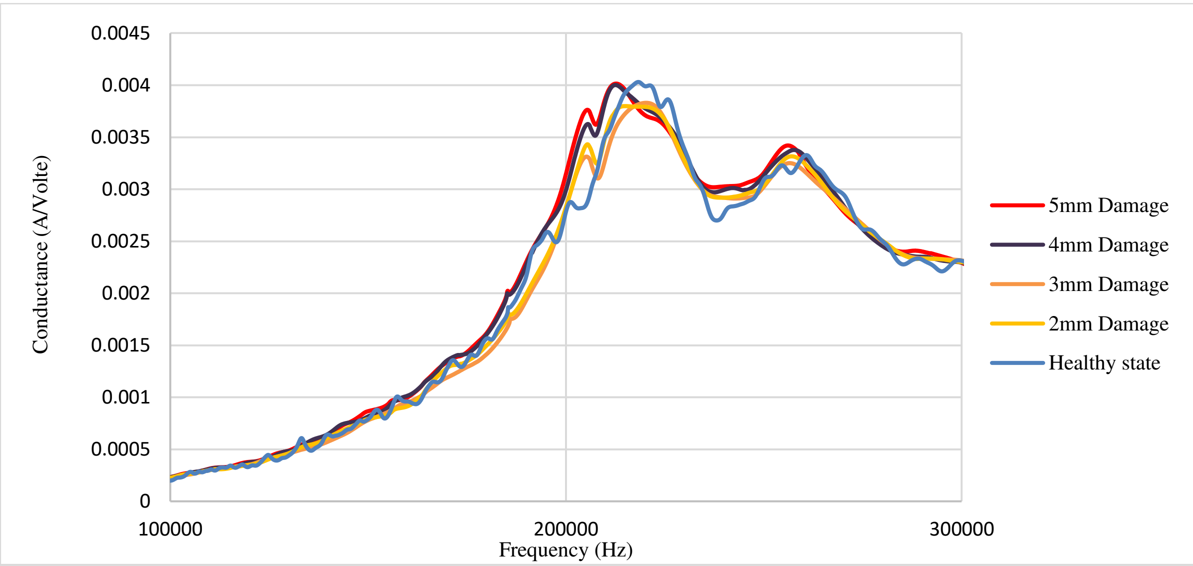

Fig.17 Comparative conductance signatures /frequency curve.

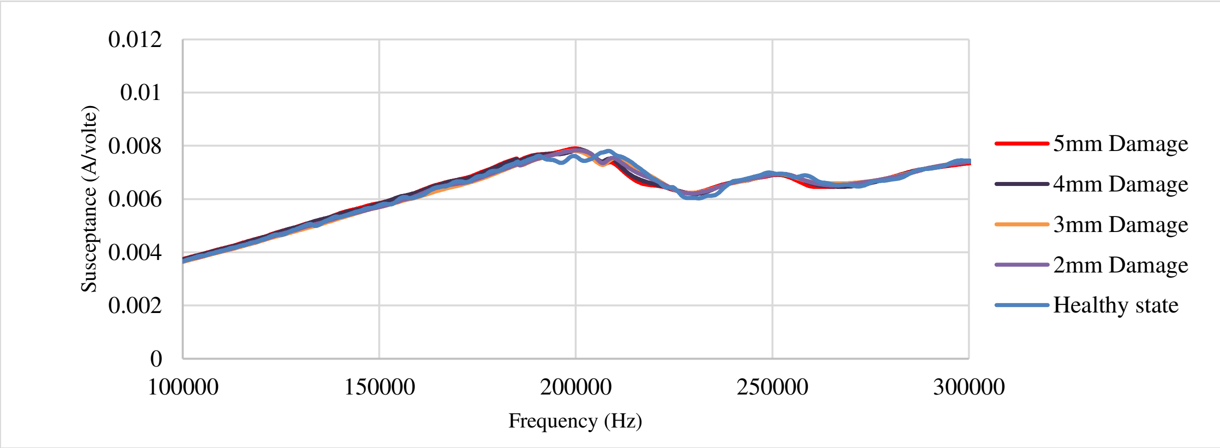

Fig.18 Comparative susceptance signatures /frequency curve

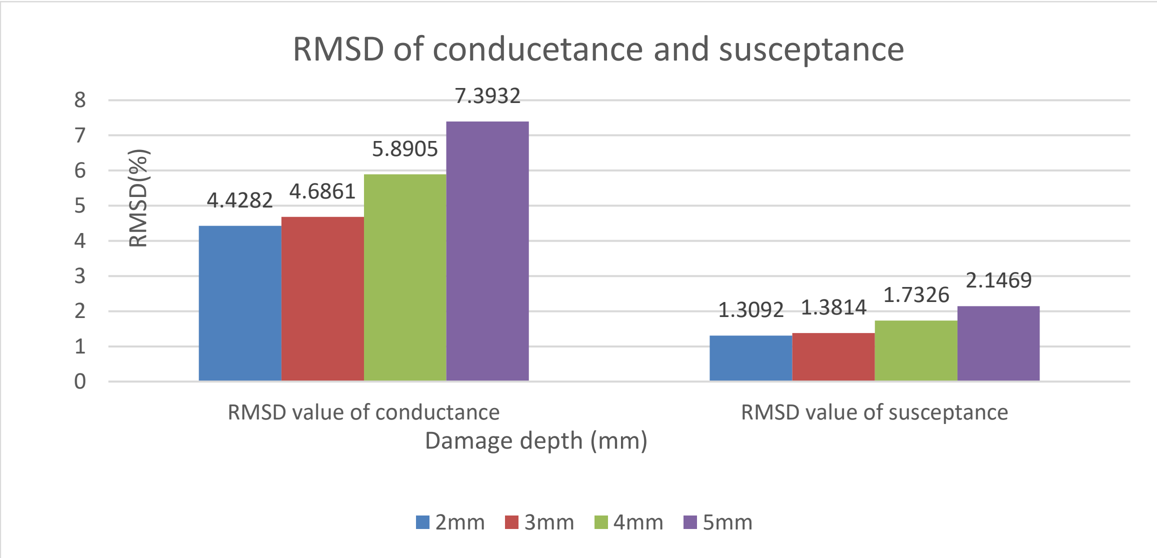

Fig.19 Percentage RMSD value of conductance and susceptance signature.

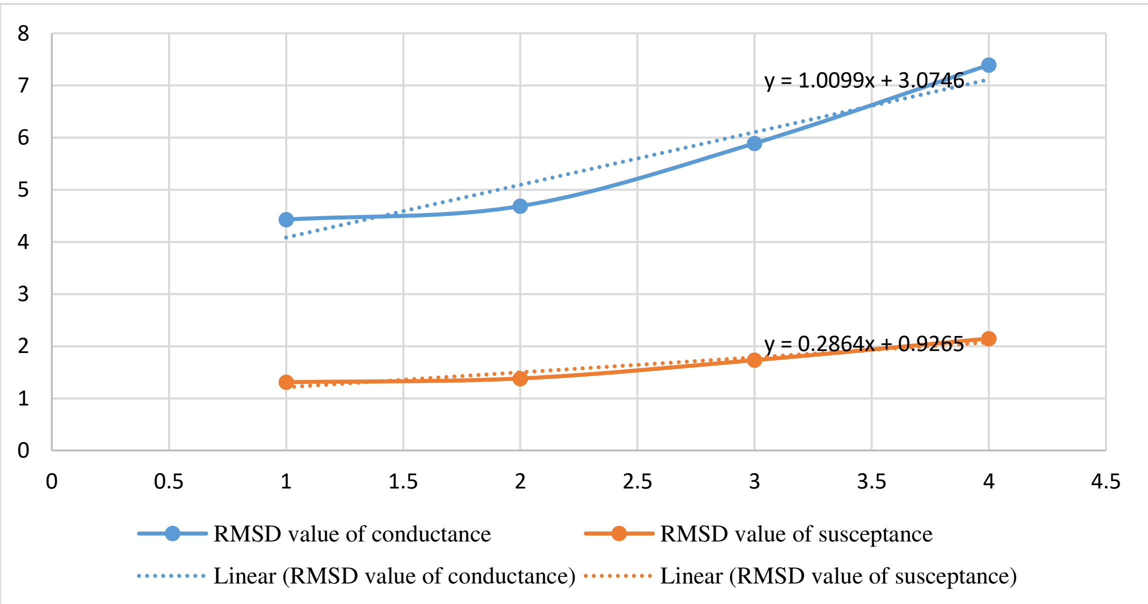

Fig.20 Equation of Percentage RMSD value of conductance and susceptance signature.

Results

A comparative result of conductance signature is in figure 17. The continuous shifting has been observed in conductance signature from baseline up to 5 mm damage. The 2mm, 3mm, 4mm, and 5mm, has been observed a continuous increase in damage then; the signature of conductance also shift towards the left side. It indicates the severity of the damage. The shifting depends upon the damage level; if the damage is more than 5 mm, then the curve may shift more on the left side.

The percentage of RMSD values also depends on damage severity. A linear function generated with the help of the percentage of RMSD values has been correlated in the form of a straight line. Generated linear function may be use damage more than 5mm of depth.

Limitations

Most of the chance is PZT patch gets broken due to its brittle nature when removed from the host structure. The PZT patch sensing zone is limited. The sensing range depends upon material shape, size, and properties of the material. Generally is a 0.4 to 2 meters length of sensing zone. Aging, mechanical, electrical, and thermal, etc., are some limitations of the PZT patch. The main restrictions in the historical structure are the originality and aesthetic view of the structure. The sandstone masonry structure contains different bonding materials such as lime mortar, etc. at this junction point, the signature is affected.

Conclusions

The historical structure is very important in culture, history, and tourism. Health monitoring is necessary for preventing the adverse effect of structure. The EMI technique is helpful to determine the incipient damage as well as damage severity for the sustainability of historical structure made of sandstone.

There are lot of restrictions on the historical structure that does not change its originality of structure. Due to this limitation a non-destructive test is useful for monitoring the health of historical structure. This technique may be directly used to monitor the health of structures within the restriction of historic structures.

The baseline of the signature is very useful for the future analysis of damage and rehabilitation of the structure. The conductance signature and susceptance signature are co-related to the strength gain and losses of the specimen.

The PZT size is tiny, so this technique does not affect the aesthetic or harm the historical structure. This technique is less time consuming.

The percentage RMSD value is used to evaluate the damage and further deterioration in the structure.

Acknowledgement The author would like to gratefully thank the dept. of civil engineering and structural engineering lab of the Motilal Nehru National Institute of Technology Allahabad, Prayagraj, India.

Funding There is no specific funding received by author(s) for this study.

Conflicts of Interest The authors declare that they have no conflicts of interest to report regarding the present study.

Author contribution Kushlendra Lal Kharwar: Writing - original draft. Anupam Rawat: Writing - review and editing. Rahul Srivastava: Review and editing.

Data availability Not applicable

Declarations

Ethical Approval Not applicable

Consent to participate Not applicable

Consent for publication Not applicable

Competing interests The authors declare no competing interests.

References

Ai, D., Zhu, H., Luo, H., & Yang, J. (2014). An effective electromechanical impedance technique for steel structural health monitoring. *Construction and Building Materials*, *73*, 97–104. https://doi.org/10.1016/j.conbuildmat.2014.09.029

Batista, H. F. M., Saba, M., & Qui, E. E. (2019). *Impact of environmental factors on the deterioration of the Wall of Cartagena de Indias*. *39*, 305–313. https://doi.org/10.1016/j.culher.2019.03.001

Belfiore, C. M., Barca, D., Bonazza, A., & Comite, V. (2013). *Application of spectrometric analysis to the identification of pollution sources causing cultural heritage damage*. 8848–8859. https://doi.org/10.1007/s11356-013-1810-y

Berrocal-olave, A., Saba, M., & Olmo-garcia, J. C. (2021). Case Studies in Construction Materials Relationship between damage and structural vulnerability in historical heritage : Case study of San Fernando de Bocachica Fort , Cartagena de Indias. *Case Studies in Construction Materials*, *15*(August), e00695. https://doi.org/10.1016/j.cscm.2021.e00695

Bhalla, S., & Soh, C. K. (2004a). *Structural Health Monitoring by Piezo-Impedance Transducers. I: Modeling*. *October*, 154–165.

Bhalla, S., & Soh, C. K. (2004b). *Structural Health Monitoring by Piezo–Impedance Transducers. II: Applications*. *October*, 166–175.

Consumption, P. (1994). *Journal of Intelligent Material Systems and Structures Coupled Electro-Mechanical Analysis of Adaptive Material Systems & mdash ; Determination of the Actuator Power Consumption and System Energy Transfer*. https://doi.org/10.1177/1045389X9400500102

Dighe, B., Singh, M. R., & Pokharia, A. K. (2020). Materials Today : Proceedings Ancient Indian techniques for sustainable and environmentally friendly decorative earthen plasters of Karla and Bhaja Caves , India. *Materials Today: Proceedings*, *32*, 536–543. https://doi.org/10.1016/j.matpr.2020.02.040

Dongyu, X., Shifeng, H., & Xin, C. (2014). Electromechanical impedance spectra investigation of impedance-based PZT and cement / polymer based piezoelectric composite sensors. *Construction and Building Materials*, *65*, 543–550. https://doi.org/10.1016/j.conbuildmat.2014.05.035

Effectiveness, T. H. E., Nano, O. F., Polymers, M., Preservation, F. O. R., Brick, H., & In, M. (2018). *CONSERVATION SCIENCE THE EFFECTIVENESS OF NANO MATERIALS AND NANO- MODIFIED POLYMERS FOR PRESERVATION OF HISTORIC BRICK MASONRY IN RASHID , EGYPT*. *9*(4), 835–846.

Fermo, P., Turrion, R. G., & Rosa, M. (2015). *RESEARCH ARTICLE A new approach to assess the chemical composition of powder deposits damaging the stone surfaces of historical monuments*. 6262–6270. https://doi.org/10.1007/s11356-014-3855-y

Korkanç, M. (2013). *Deterioration of different stones used in historical buildings within Nigde province , Cappadocia*. *48*, 789–803. https://doi.org/10.1016/j.conbuildmat.2013.07.033

Labus, M., & Bochen, J. (2012). *Sandstone degradation : an experimental study of accelerated weathering*. 2027–2042. https://doi.org/10.1007/s12665-012-1642-y

Mahesh, S., Kasthurba, A. K., & Patil, M. V. (2021). Case Studies in Construction Materials Characterization and assessment of stone deterioration on Heritage Buildings. *Case Studies in Construction Materials*, *15*(September), e00696. https://doi.org/10.1016/j.cscm.2021.e00696

Manohar, S., Bala, K., Santhanam, M., & Menon, A. (2020). Characteristics and deterioration mechanisms in coral stones used in a historical monument in a saline environment. *Construction and Building Materials*, *241*, 118102. https://doi.org/10.1016/j.conbuildmat.2020.118102

Martínez-garrido, M. I., & Ergenc, D. (2016). *Sensors and Actuators A : Physical Wireless monitoring to evaluate the effectiveness of roofing systems over archaeological sites*. *252*, 120–133. https://doi.org/10.1016/j.sna.2016.10.038

Maurya, K. K., Rawat, A., & Shanker, R. (2022a). Materials Today : Proceedings Health monitoring of cracked concrete structure by impedance approach. *Materials Today: Proceedings*, *xxxx*. https://doi.org/10.1016/j.matpr.2022.03.053

Maurya, K. K., Rawat, A., & Shanker, R. (2022b). *Review Article on Condition Assessment of Structures Using Electro-Mechanical Impedance Technique*. https://doi.org/10.32604/sdhm.2022.015732

Maurya, K. K., Sonker, T., & Rawat, A. (2020). Materials Today : Proceedings Sustainable concrete construction by microorganism and monitoring using EMI technique : A review. *Materials Today: Proceedings*, *32*, 670–676. https://doi.org/10.1016/j.matpr.2020.03.169

Mishra, M. (2021). Machine learning techniques for structural health monitoring of heritage buildings : A state-of-the-art review and case studies. *Journal of Cultural Heritage*, *47*, 227–245. https://doi.org/10.1016/j.culher.2020.09.005

Moharana, S., & Bhalla, S. (2014). International Journal of Solids and Structures A continuum based modelling approach for adhesively bonded piezo-transducers for EMI technique. *International Journal of Solids and Structures*, *51*(6), 1299–1310. https://doi.org/10.1016/j.ijsolstr.2013.12.022

Natarajan, N. (2022). *Effects of air pollution on monumental buildings in India : An overview*. 29399–29408.

Negi, P., Chakraborty, T., Kaur, N., & Bhalla, S. (2018). Investigations on effectiveness of embedded PZT patches at varying orientations for monitoring concrete hydration using EMI technique. *Construction and Building Materials*, *169*, 489–498. https://doi.org/10.1016/j.conbuildmat.2018.03.006

Ortega-calve, J. J., & Ariiio, X. (1995). *Factors affecting the weathering and colonization of monuments by phototrophic microorganisms*. *167*, 329–341.

Pandey, A. K., & Kumar, V. (2015). *IMPACT OF ENVIRONMENTAL POLLUTION ON HISTORICAL MONUMENTS OF INDIA : CONSERVATION PROBLEMS AND REMEDIAL MEASURES*. *17*(1), 2015.

Pinna, D., Bracci, S., Magrini, D., Salvadori, B., Andreotti, A., & Colombini, M. P. (2022). Deterioration and discoloration of historical protective treatments on marble. *Environmental Science and Pollution Research*, 20694–20710. https://doi.org/10.1007/s11356-021-16879-8

Prakash, A., & Rajdeo, M. (2019). Vibrational Spectroscopy Spectroscopic and chromatographic investigation of the wall painted surfaces of an 18th century Indian temple , New Delhi. *Vibrational Spectroscopy*, *104*(June), 102947. https://doi.org/10.1016/j.vibspec.2019.102947

Prasad, A., Pallav, K., & Singh, D. K. (2019). *Seismic Behaviour of 17th Century Khusro Tomb Due to Site-Specific Ground*. *March*.

https://doi.org/10.2174/1874149501913010026

Priya, C. B., Saravanan, T. J., Balamonica, K., Gopalakrishnan, N., & Mohan, A. R. (2018). EMI based monitoring of early-age characteristics of concrete and comparison of serial / parallel multi-sensing technique. *Construction and Building Materials*, *191*, 1268–1284. https://doi.org/10.1016/j.conbuildmat.2018.10.079

Ruedrich, J., & Bartelsen, T. (2011). *Moisture expansion as a deterioration factor for sandstone used in buildings*. 1545–1564. https://doi.org/10.1007/s12665-010-0767-0

Saba, M., Quiñones-bolaños, E. E., Liliana, A., & López, B. (2018). Review article A review of the mathematical models used for simulation of calcareous stone deterioration in historical buildings. *Atmospheric Environment*, *180*(September 2017), 156–166. https://doi.org/10.1016/j.atmosenv.2018.02.043

Saltik, E. N. (2010). *" Investigations on sandstone deterioration ". January*.

Saravanan, T. J., & Chauhan, S. S. (2022). Study on pre-damage diagnosis and analysis of adhesively bonded smart PZT sensors using EMI technique. *Measurement*, *188*(June 2021), 110411. https://doi.org/10.1016/j.measurement.2021.110411

Shanker, R., Bhalla, S., Gupta, A., & Kumar, M. P. (2011). *Journal of Intelligent Material Systems and Structures*. https://doi.org/10.1177/1045389X11414219

Silva, L. F. O., Oliveira, M. L. S., Neckel, A., Milanes, C. B., Bodah, B. W., Cambrussi, L. P., & Dotto, G. L. (2022). *Urban Climate Effects of atmospheric pollutants on human health and deterioration of medieval historical architecture (North*. *41*(November 2021). https://doi.org/10.1016/j.uclim.2021.101046

Sirohi, J., & Chopra, I. (2000). *Journal of Intelligent Material Systems and Structures*. https://doi.org/10.1106/8BFB-GC8P-XQ47-YCQ0

Spectus, C. O. N. (2010). *Study of Sticky Rice - Lime Mortar Technology*. *43*(6).

Ural, A., & Dog, A. (2008). *Turkish historical arch bridges and their deteriorations and failures*. *15*, 43–53. https://doi.org/10.1016/j.engfailanal.2007.01.006

Varotsos, C., Tzanis, C., & Cracknell, A. (2009). *The enhanced deterioration of the cultural heritage monuments due to air pollution*. 590–592. https://doi.org/10.1007/s11356-009-0114-8

Vidović, K., Hočevar, S., Menart, E., Drventić, I., Grgić, I., & Kroflič, A. (2022). Impact of air pollution on outdoor cultural heritage objects and decoding the role of particulate matter : a critical review. In *Environmental Science and Pollution Research*. Springer Berlin Heidelberg. https://doi.org/10.1007/s11356-022-20309-8

Wasserman, R. I. (2021). *applied sciences Deterioration of Sandstone in the Historical and Contemporary Sea Walls upon the Impact of the Natural and Man-Made Hazards*.